CHARACTERIZING THE COMPONENTS IN TWO FERROAN ANORTHOSITE CLASTS WITHIN SAMPLE 60016. M.A. Torcivia[1] and C.R. Neal[2], [1,2]University of Notre Dame, Notre Dame IN, 46556; ([1]mtorcivi@nd.edu; [2]cneal@nd.edu)

Introduction: The ferroan anorthosite suite (FAS) represents some of the oldest remnants of the primordial lunar crust that we have available to study. Understanding the FAS has important implications for defining the earliest history of the Moon – especially regarding its initial differentiation. Lunar sample 60016 is described as an ancient regolith breccia that contains ferroan anorthosite clasts [16]. One of these FAS clasts (designated clast 3A) yields a Sm-Nd crystallization age of 4.302±0.028 Ga that is concordant with both Rb-Sr and Ar-Ar chronometers [1]. This is a relatively young age for a sample of the early lunar crust, but young Sm-Nd ages for FAS material are not unusual [2,3]. However, these young FAS ages challenge the classic model of lunar magma ocean (LMO) crystallization because liquid would need to be present for >200 m.y. External factors, such as an insulating lid coupled with tidal heating [4], have been proposed to reconcile the purported long LMO crystallization period.

Two thin sections of 60016 FAS clasts, 60016,98 and 60016,229 (Clast 3A), have been examined using in-situ analysis methods to characterize the individual minerals to determine whether these components are consistent with an LMO parentage by comparing them to established LMO models [4-8].

Methods: Each thin section was imaged in cross polarized (XPL), plane polarized (PPL), and reflected light (RF). Complete photomicrographs of each thin section were stitched together using the Microsoft Image Composit Editor (ICE) program. These images provide context to the subsequent in-situ analyses as well as to serve as a navigation map for those analyses. Major and minor elements were analyzed using a Cameca SX-50 electron microprobe at the University of Notre Dame. Compositions of plagioclase, pyroxene, and olivine were obtained. Trace element data for plagioclase were gathered via laser ablation (LA) ICP-MS at the MITERAC facility at Notre Dame. A NIST-612 glass [9] served as the external standard, while CaO content from the electron microprobe served as the internal standard for each laser datum. Data were reduced using the GLITTER software package [10]. Equilibrium liquids were calculated using the partition coefficients of [11] for plagioclase.

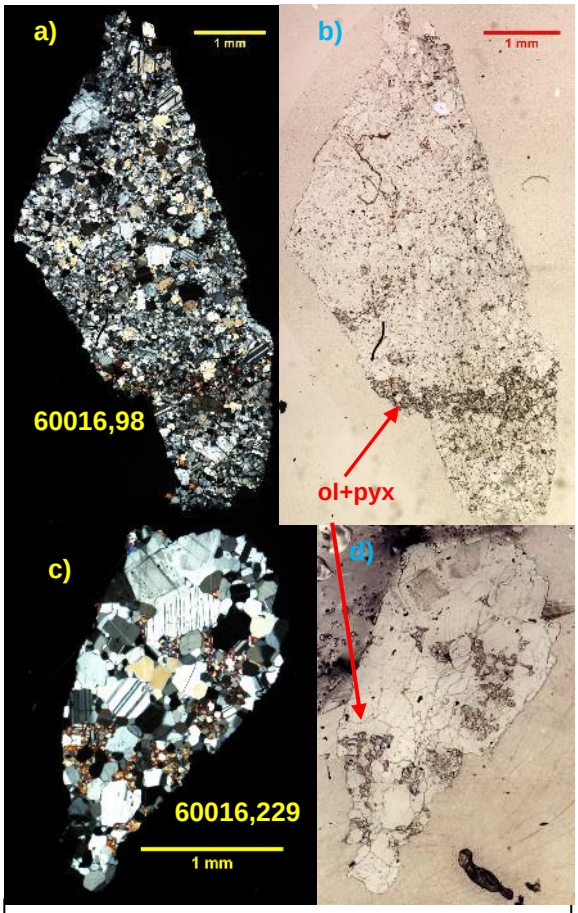

Figure 1: XPL (a,c) and PPL (b,d) photomicrographs of the two thin sections of 60016 studied here. Note the defined triple junctions present throughout section 229 (c), and the localized veins/blebs of mafic material (b,d).

Results and Discussion:

Petrography: The thin sections of 60016 studied here represent typical FAS samples. They are plagioclase-rich with minor pyroxene and olivine. The pyroxene and olivine grains are much smaller than the plagioclase grains and mostly occur as localized veins or blebs between plagioclase grains rather than dispersed throughout the sample (**Fig. 1**). The samples are severely brecciated/cataclasized which obscures the original relationship between the individual grains. Section ,98 additionally contains some granulitic anorthosite (**Fig 1**), while section ,229 plagioclase grains often contain triple junctions indicating that these grains have experienced textural re-equilibration.

EMP Analysis: Plagioclases in 60016 are anorthite (An)-rich, but display a relatively large range in anorthtite from ~An_{90}-An_{97} (**Fig. 2**). In both thin sections, the cores of the plagioclase grains tend to be more An-rich than their corresponding rims and show a negative correlation with FeO. This is consistent with an original igneous fractionation trend of plagioclase grains crystallizing out of an evolving melt. The pyroxenes in these samples include pigeonite, augite, and orthopyroxene

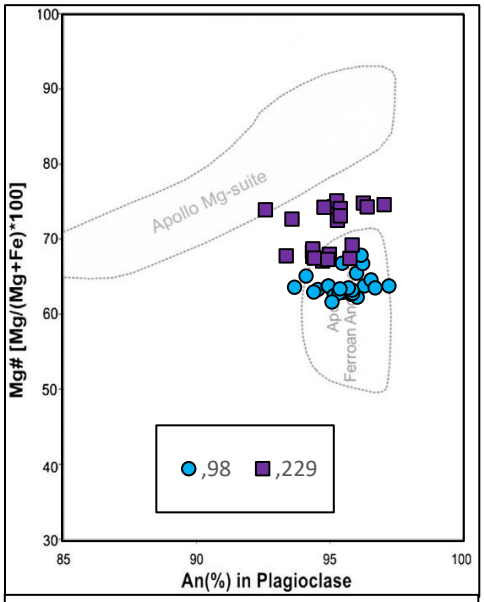

Fig. 2: An vs. Mg# in 60016 pyroxenes. The higher Mg# groups in both sections = augites.

(**Fig. 3**). The pyroxenes in ,229 are more Mg-rich (average Mg# of 71) than those found in ,98 (average Mg# of 64, **Fig. 2, 3**). Section ,98 contains only pigeonite as the low-Ca pyroxene phase (**Fig. 3**).

LA-ICP-MS Analysis: The REE in the plagioclase grains are slightly more enriched than some other FAS samples [eg. 12-14]. The concentrations of the REE in ,229 exhibit a narrower range than those in section ,98 (**Fig. 4a**). The compositional similarity between individual grains, coupled with the texture in ,229, suggests there has been some re-equilibration following a reheating event. The corresponding equilibrium liquids for these plagioclases (**Fig. 4b**) reflect a fairly significant range in concentration between individual grains, however, section ,229 is generally more enriched in the REE than ,98. If we are to assume that the pyroxenes co-crystallized with plagioclase, then the plagioclase which crystallized with more magnesian pyroxenes (229) should yield more primitive equilibrium liquids than those plagioclases that crystallized with more ferroan pyroxenes (,98) (**Fig. 2, Fig. 3**). The opposite of this is reflected in the trace element chemistry of these plagioclase grains (**Fig.4**).

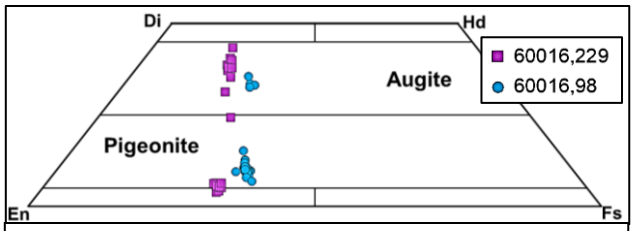

Figure 3: Pyroxene compositions for each thin section. Note the distinct compositional groups found in each section.

Conclusions and Future Work: Lunar samples 60016,98 and 60016,229 are ferroan anorthosite suite samples that – while similar in plagioclase composition – contain distinct populations of pyroxene grains. Additionally, the texture of section ,229 indicate that it has experienced some degree of re-equilibration to produce marked triple junction features. It appears that this produced re-equilibration of the REE and probably the Sm-Nd age, which is concordant with Rb-Sr and Ar-Ar ages – systems that are more easily reset than Sm-Nd. Future work will compare the data gathered here to modeled LMO evolution paths [4-8] to determine provenance for individual components in these sections.

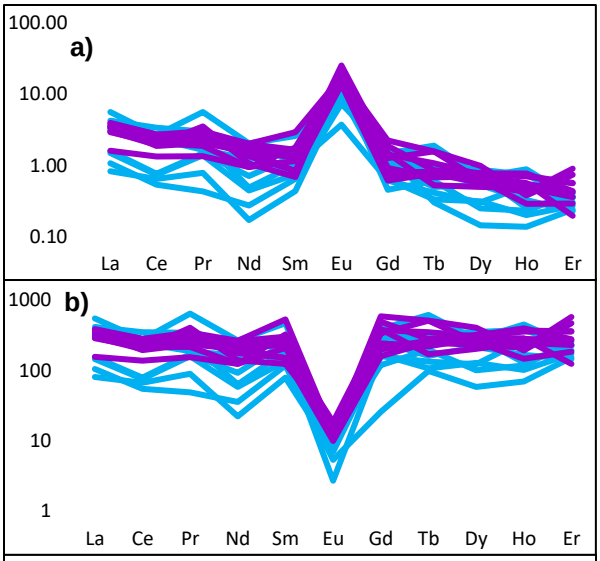

Figure 4: a) Plagioclase grain REE concentrations normalized to chondrite [15] b) corresponding equilibrium liquids for the plagioclase grains in (a). For both plots, blue represents grains from ,98 while purple represent grains from ,229

Acknowledgements: This work is supported by NASA grant 80NSSC17K0467.

References: [1] Marks et al. (2019) *JGR:Planets* 124, 2465-2481; [2] Borg et al. (1999) *GCA* 63, 2679-2691. [3] Borg et al. (2011) *Nature* 477, 70. [4] Elkins-Tanton et al. (2011) *EPSL* 304, 326-336. [5] Snyder et al. (1992) *GCA* 56, 3809-3823. [6] Lin et al. (2017) *EPSL* 471, 104-116. [7] Charlier et al. (2018) *GCA* 234, 50-69. [8] Rapp, J.F. and Draper D.S. (2018) *MaPS* 53, 1432-1455. [9] Pearce N. et al. (1997) *Geostds. Nwslet.* 21, 115-144. [10] van Achterbergh E. et al. (2001) *MSA, Short Course* 29, 239–243. [11] Sun et al. (2017) *GCA* 206, 273-295. [12] Torcivia, M.A. & Neal, C.R. (2017) *LPSC*, abstract #1480 [13] Torcivia, M.A. & Neal, C.R. (2018) *LPSC*, abstract #1331 [14] Torcivia, M.A. & Neal, C.R. (2019) *LPSC*, abstract #2536 [15] Anders E. & Grevesse N. (1989) *GCA* 53, 197-214. [16] McKay D. et al. (1986) *PLPSC* 16. *JGR*. 91, D277-D303.